



Title	Float zone growth and spectral properties of Cr,Nd:CaYAIO4 single crystals
Author(s)	Ueda, Aki; Higuchi, Mikio; Yamada, Daiki; Namiki, Sho; Ogawa, Takayo; Wada, Satoshi; Tadanaga, Kiyoharu
Citation	Journal of Crystal Growth, 404, 152-156 https://doi.org/10.1016/j.jcrysgr.2014.07.027
Issue Date	2014-10-15
Doc URL	http://hdl.handle.net/2115/57424
Type	article (author version)
File Information	paper_revised.pdf



[Instructions for use](#)

Float zone growth and spectral properties of Cr,Nd:CaYAlO₄ single crystals

Aki Ueda^a, Mikio Higuchi^{a,b,*}, Daiki Yamada^a, Sho Namiki^b, Takayo Ogawa^b,

Satoshi Wada^b, Kiyoharu Tadanaga^a

^aFaculty of Engineering, Hokkaido University, Sapporo 060-8628, Japan

^bRIKEN, Wako 351-0198, Japan

*Corresponding author

Phone: +81-11-706-6573

E-mail: hig@eng.hokudai.ac.jp

Abstract

Cr,Nd:CaYAlO₄ single crystals were grown by the floating zone method and their spectroscopic properties were investigated. Many voids were observed in the crystals grown with a stoichiometric feed rod even at a relatively low growth rate of 2.5 mm/h, while a void-free crystal was grown at the same growth rate using a feed rod the composition of which was Y-rich to Ca. These results indicate that voids were

attributable to constitutional supercooling due to the segregation of main constituents caused by the difference in congruent and stoichiometric compositions. The as-grown crystals were deep red and showed strong absorption in the wavelength region of 320-600 nm. The absorption cross section for σ -polarization at 430 nm, where Cr,Nd:YAG has the maximum absorption, is about $1160 \times 10^{-20} \text{ cm}^2$, which is 165 times as large as that of Cr,Nd:YAG. By pumping at 400 nm, which is a part of the absorption band of Cr^{3+} , Cr,Nd:CaYAlO₄ showed fluorescence bands around 900 nm and 1080 nm by Nd^{3+} indicating energy transfer from Cr^{3+} to Nd^{3+} in the crystal. Cr,Nd:CaYAlO₄ single crystals are therefore one of the promising gain media for solar-pumped solid state laser systems.

Highlights

- Cr,Nd:CaYAlO₄ single crystals were grown by the floating zone method.
- Void formation is attributable to the segregation between Ca and Y species.
- Absorption cross-section of Cr,Nd:CaYAlO₄ for σ -polarizaion was about $1160 \times 10^{-20} \text{ cm}^2$.
- Emission bands of Nd³⁺ were observed with the excitation at 400 nm.

Keywords

- A1 Defects
- A2 Floating zone technique
- B1 Aluminates
- B3 Solid state lasers

1. Introduction

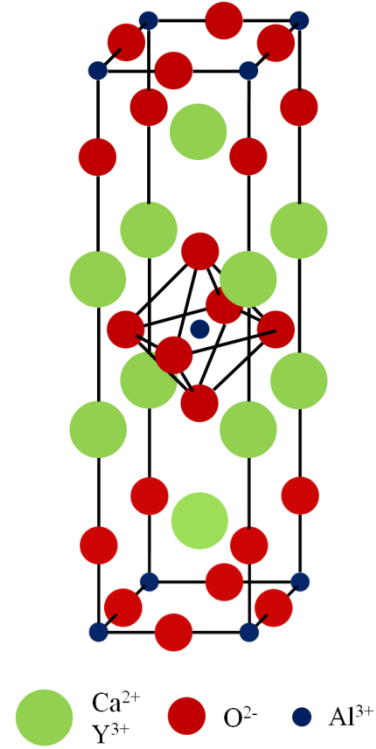
Depletion of fossil fuels will be one of the most serious problems in the future even though mining technologies are progressing, and efficient utilization of solar energy is therefore strongly required from the viewpoint of development of sustainable energy sources. Solar-pumped laser is one of the effective systems to utilize solar energy. Yabe et al. suggested a magnesium refining system using solar-pumped laser system [1] and succeeded to obtain an output of 80 W with YAG ceramic as a gain medium by pumping with converged solar radiation [2]. Hydrogen production using metal nanoparticles [3] or photocatalysts [4], and transmission of solar energy to the ground from space [5] are also possible applications of the solar-pumped lasers.

A number of candidate materials such as Nd-doped glass [6, 7] and oxide single crystals [8-10] have so far been developed as the gain media for solar-pumped lasers. Cr,Nd:YAG is one of the most investigated media [11], and the transparent YAG ceramic is mainly used in recent studies [12]. However, absorption of Cr,Nd:YAG around 500 nm which corresponds to the wavelength of solar radiation peak and the absorption cross section are relatively small even at the absorption peak wavelength. In addition, the garnet structure has four-fold coordination site and chromium can occupy the site as a tetravalent ion, Cr^{4+} , which shows a broad absorption band in the

near-infrared region where Nd^{3+} emission bands are present resulting in reduced lasing performance [13].

In order to overcome these problems, we focused on CaYAIO_4 as a host crystal for Cr^{3+} and Nd^{3+} . The structure of CaYAIO_4 is illustrated in Fig.

1. CaYAIO_4 adopts the K_2NiF_4 type structure, in which no tetrahedral site exists, and nine-fold coordinated Y site and six-fold coordinated Al site can be substituted by Nd^{3+} ion and Cr^{3+} ion, respectively. Due to the random distribution of Ca^{2+}



and Y^{3+} in the structure [14], coordination environment of Cr^{3+} is diversified, and broadening of the absorption band of Cr^{3+} is consequently expected. In previous studies, laser oscillation was reported using a $\text{Nd}:\text{CaYAIO}$ single crystal [15-17] and growth of CaYAIO_4 single crystals doped with other rare earth ions were investigated [18-22]. $\text{Cr}:\text{CaYAIO}_4$ was also synthesized and broad absorption bands in the visible region were observed [22, 23]. However, there has been no report on the growth and spectroscopic properties of $\text{Cr,Nd}:\text{CaYAIO}_4$ single crystals.

In this study, we tried float zone growth of $\text{Cr,Nd}:\text{CaYAIO}_4$ single crystal to

establish adequate growth conditions to obtain high quality single crystals which can be used as a laser medium and revealed spectroscopic properties of Cr,Nd:CaYAlO₄. On the basis of the obtained results, the potentiality of Cr,Nd:CaYAlO₄ single crystals as a solar pumped laser medium is discussed.

2. Experimental procedure

CaCO₃ (99.99%), Y₂O₃ (99.99%), Nd₂O₃ (99.9%), Al₂O₃ (99.99%) and Cr₂O₃ (99.98%) were used as starting materials. They were weighed according to the compositions shown in Table 1 and mixed in an alumina mortar with ethanol, followed

by calcination in

air at 1000 °C for

10 h. The calcined

powder was ground

and pressed into a

rod under a

hydrostatic

Sample	Composition
Stoichiometry	Ca(Y _{0.99} Nd _{0.01})(Al _{0.999} Cr _{0.001})O ₄
Y-rich 0.5 mol% vs. Ca	Ca _{0.9925} (Y _{0.99} Nd _{0.01}) _{1.005} (Al _{0.999} Cr _{0.001})O ₄
Al-rich 0.5 mol% vs. Y	Ca(Y _{0.99} Nd _{0.01}) _{0.995} (Al _{0.999} Cr _{0.001}) _{1.005} O ₄

pressure of 100 MPa. The rod was sintered in air at 1400 °C for 10 h and a feed rod was

thus obtained. Cr,Nd:CaYAlO₄ single crystals were grown using an image furnace with

double ellipsoidal mirrors (SC-N35HD-L, NEC, infrared source: halogen lamp of 1.5 kW). The growth atmosphere was O₂, air, air / N₂ mixed gas, CO₂, or N₂ stream (2 L/h). The growth rate was 2.5-5 mm/h, and the rotation rate was 30-60 rpm for the seed crystal and 5 rpm for the feed.

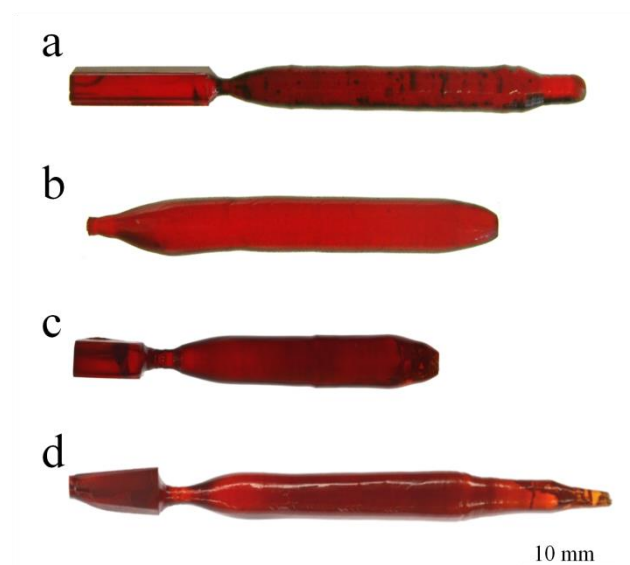
A polarizing microscope (BX51, OLYMPUS and SZH-ILLB, OLYMPUS) was used to evaluate the quality of the grown crystals. Initial and end portions of the grown crystals were cut into discs and both sides of the discs were polished to be mirror finish. An X-ray diffractometer (RINT-2000 Ultima, Rigaku) was used to determine the lattice parameters of the grown crystals.

Polarized absorption spectra of the Cr,Nd:CaYAlO₄ were measured using a sample in which the c-axis was parallel to the surface with a spectrophotometer (UV-VIS-NIR scanning spectrophotometer, Shimadzu). Emission spectra were also measured with a fluorescence spectrophotometer (Fluolog®-3, HORIBA).

3. Results and discussion

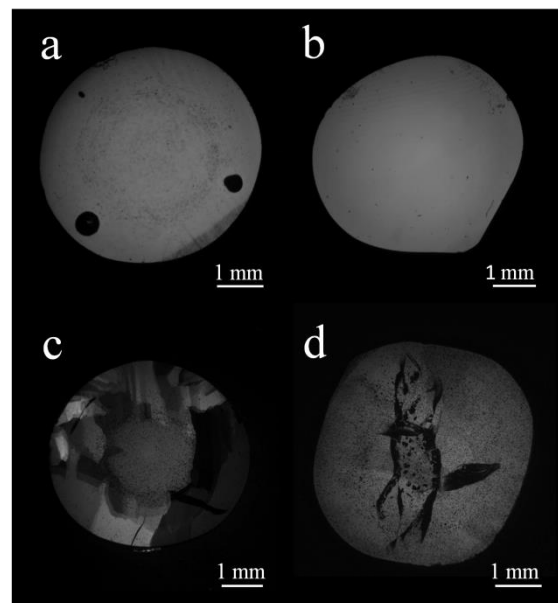
3.1. Crystal growth

Cr,Nd:CaYAlO₄ single crystals grown in various atmospheres are



shown in Fig. 2. The growth rate and the rotation rate for every crystal were 2.5 mm/h and 30 rpm, respectively. The as-grown crystals were transparent and deep red in whole. Bubbles of about 1 mm in diameter were observed in the crystals grown in O₂ stream as shown in Fig. 2a. The cause of the bubble formation is not yet well known, but pores in the feed rods might be entrained in the molten zone and be trapped at the growth interface. Transparency of the crystal grown in the N₂ stream (Fig. 2d) was appreciably lower than those of other crystals grown under different atmospheres. Polarizing microphotographs of the initial portions of the single crystals grown in different atmospheres are shown in Fig. 3. Many voids were found in the central region of every

crystal. Much more voids were observed in the crystals grown in the N₂ stream and were responsible to the decrease in the transparency of this crystal. The number of voids increased with the progression of crystal growth in every crystal. It was expected that there was some relationship

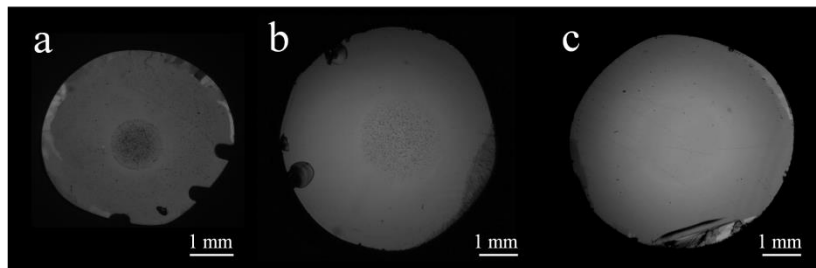


between the oxygen partial pressure and the crystal quality; however, no evident dependence was observed. These results are similar to the previous report by Wang, et al.

[18]. Although the void formation was not completely suppressed only by controlling the oxygen partial pressure, air was found to be appropriate to grow a better crystal and following results are accordingly obtained by using air as a growth atmosphere.

Fig. 4 shows polarizing microphotographs of the end portions of the crystals grown at different growth rates and rotation rates. Many voids were found in the central

regions of the crystal
grown at 5 mm/h;
however, the number



of voids was appreciably reduced in the crystal grown at 2.5 mm/h. Furthermore, increase in the rotation rate from 30 rpm to 60 rpm was also effective to reduce the number of voids.

On the basis of above-mentioned results, constitutional super-cooling due to segregation of some chemical species could be responsible to the formation of voids because lower growth rate and higher rotation are effective. In addition this consideration is also supported by the fact that the number of voids increased along the growth direction. In order to identify the chemical species that segregates at the growth interface, lattice parameters of the initial and end portions of the grown crystal (growth rate: 2.5 mm/h, rotation rate: 30 rpm, growth atmosphere: air) were determined from the

X-ray powder diffraction patterns using a least square method. The results are shown in

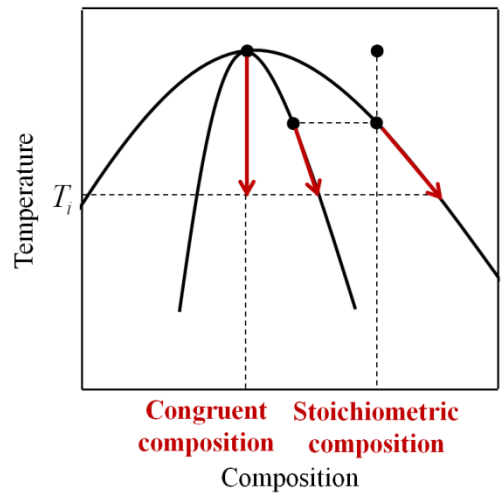
Table 2. The lattice parameters of the end portion are slightly larger than that of the

	Lattice parameter	
	a-axis [Å]	c-axis [Å]
Initial portion	3.6455(2)	11.8750(6)
End portion	3.6471(2)	11.8813(6)

Nd or Cr could be the species that segregate since the ionic radii of Nd^{3+} and Cr^{3+} are larger than those of Y^{3+} and Al^{3+} , respectively. However, there was no significant difference in the absorption coefficients of the initial and end portions of the crystal and these elements can be excluded. If there is an appreciable difference between the stoichiometric and congruent compositions the elements of the host crystal can be responsible to the segregation.

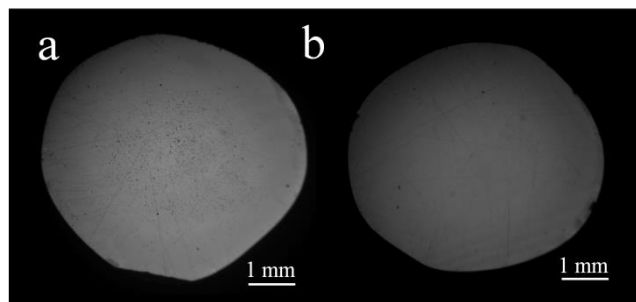
As illustrated in Fig. 5, if the congruent composition is shifted from the stoichiometric one towards an end member

the ionic radius of which is smaller than that of the counter ion, the increase in the lattice parameter can be explained. On the basis of the ternary phase diagram for the $\text{CaO-Y}_2\text{O}_3\text{-Al}_2\text{O}_3$ system [24], possible



combinations are Al-Y and Y-Ca. The combination of Al-Ca can be excluded since both charges and crystallographic sites are different. Single crystals were accordingly grown using feed rods in which the chemical compositions are Y-rich for Ca ($Y/Ca = 1.005/0.9925$) and Al-rich for Y ($Al/Y = 1.005/0.995$). Polarizing microphotographs of the end portions are shown in Fig. 6. While the number of voids in the crystal grown

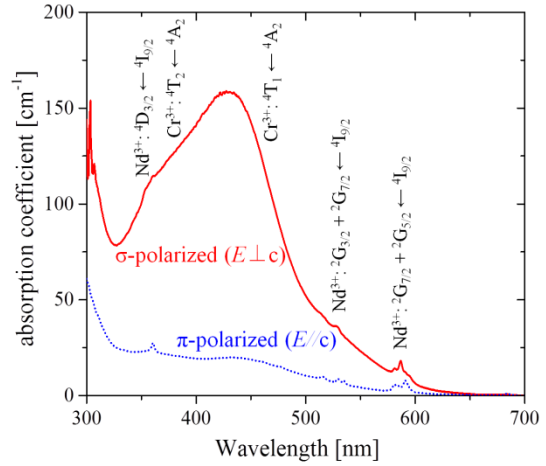
from the feed rod with the Al-rich composition was as many as that in the crystal of the composition, no void was observed in the crystal grown from the



Y-rich composition. The quality of the crystal with Y-rich grown at a rotation rate of 30 rpm, was much higher than that of the stoichiometric crystal grown at 60 rpm with the same growth rate of 2.5 mm/h. These results strongly support the anticipation that the void formation is attributable to constitutional super-cooling that is based on segregation between Ca and Y species. Although the true congruent composition of this material is not known, the composition is expected to be around $Ca_{0.9925}(Y,Nd)_{1.005}(Al,Cr)O_4$. If the true congruent composition is determined, higher growth rate than 2.5 mm/h will be possible to obtain high quality Cr,Nd:CaYAlO₄ single crystals.

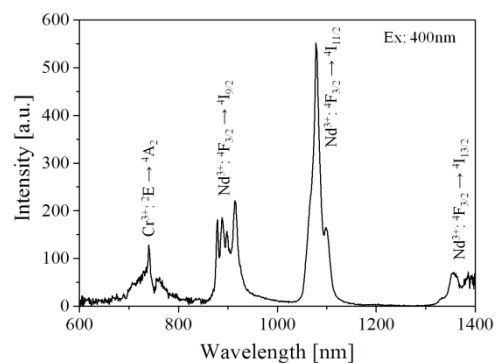
3.2. Spectroscopic properties

Fig. 7 shows polarized absorption spectra of the Cr,Nd:CaYAlO₄ single crystal in the visible region. Strong, broad absorption bands of Cr³⁺ are observed from about 300 nm to 600 nm for the



σ -polarization. As expected from the crystal structure in which AlO₆ octahedra form layers perpendicular to the c-axis, σ -polarized ($E \perp c$) absorption of Cr³⁺ is larger than the π -polarized ($E // c$) absorption. In contrast, the absorption of Nd³⁺ was independent on the polarization. This is because Nd³⁺ ions substitute the Y-site, in which large anisotropy is not expected as in the Al-site. At 430 nm, which corresponds to the absorption peak of Cr,Nd:YAG, σ -polarized absorption cross-section of Cr,Nd:CaYAlO₄ is about $1160 \times 10^{-20} \text{ cm}^2$, which is as 165 times large as that of Cr,Nd:YAG. The absorption peak wavelength of Cr,Nd:CaYAlO₄ (428 nm)

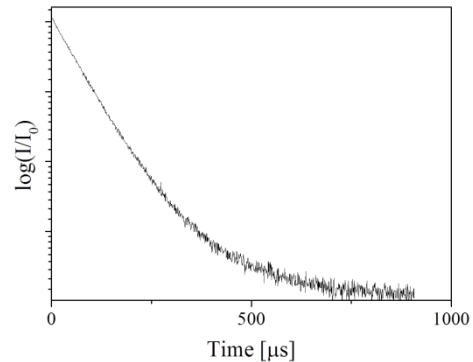
does not correspond to that of the peak wavelength of the solar radiation (~500 nm); however, the absorption coefficient



of Cr,Nd:CaYAlO₄ at 500 nm is about 50 cm⁻¹, which is practically enough for pumping. In addition, appreciable absorption was not observed in the near infrared region, where emission bands of Nd³⁺ exist.

Fig. 8 shows emission spectrum of the Cr,Nd:CaYAlO₄ single crystal. Fluorescence bands of Nd³⁺ was observed around 900 nm, 1080 nm and 1400 nm by excitation at 400 nm, where only absorption of Cr³⁺ is present. The fluorescence lifetime which was measured with 370 nm excitation is shown in Fig. 9. Although a little afterglow component was present, the fluorescence lifetime of the Cr,Nd:CaYAlO₄ single crystal

(growth atmosphere: air, growth rate: 2.5 mm/h, rotation rate: 30 rpm) is 132 μs. The fluorescence spectrum and lifetime are similar to the previous studies [15, 17]. These results indicate that energy



transfer from Cr³⁺ to Nd³⁺ occurs in the Cr,Nd:CaYAlO₄ single crystal.

4. Conclusion

In this study, we focused on Cr,Nd:CaYAlO₄ as a candidate of gain media for solar-pumped laser, and grew Cr,Nd:CaYAlO₄ single crystals by the floating zone

method. In order to obtain a high-quality crystal following growth conditions were examined: growth atmosphere, growth rate, rotation rate, and compositions of the feed rod. Lower growth rate, higher rotation rate and air atmosphere were effective to improvement the crystal quality, and a void free Cr,Nd:CaYAlO₄ single crystal was obtained by using a feed rod with the Y-rich composition (Ca/Y = 0.9925/1.005). Void formation is attributable to constitutional super-cooling based on the segregation between Ca and Y species. From the polarized absorption spectra of the Cr,Nd:CaYAlO₄, the σ -polarized absorption cross-section of Cr,Nd:CaYAlO₄ is $1160 \times 10^{-20} \text{ cm}^2$, which is as 165 times large as that of Cr,Nd:YAG at 430 nm. Emission bands of Nd³⁺ were observed around 900 nm, 1080 nm and 1400 nm with the excitation at 400 nm indicating energy transfer from Cr³⁺ to Nd³⁺ in the Cr,Nd:CaYAlO₄ single crystal. The fluorescence lifetime was 132 μs . For all of these reasons, Cr,Nd:CaYAlO₄ single crystals are a promising material as a gain medium for solar-pumped laser systems.

References

- [1] T. Yabe, S. Uchida, K. Ikuta, K. Yoshida, C. Baasandash, M.S. Mohamed, Y. Sakurai, Y. Ogata, M. Tuji, Y. Mori, Y. Satoh, T. Ohkubo, M. Murahara, A. Ikesue, M. Nakatsuka, T. Saiki, S. Motokoshi, C. Yamanaka, *J. Appl. Phys.*, 89 (2006) 261107, doi: 10.1063/1.2423320
- [2] T. Yabe, B. Bagheri, T. Ohkubo, S. Uchida, K. Yoshida, T. Funatsu, T. Oishi, K. Daito, M. Ishioka, N. Yasunaga, Y. Sato, C. Baasandash, Y. Okamoto, K. Yanagitani, *J. Appl. Phys.*, 104 (2008) 083104, doi: 10.1063/1.2998981
- [3] T. Okada, T. Saiki, S. Taniguchi, T. Ueda, K. Nakamura, Y. Nichikawa, Y. Iida, *ISRN Renewable Energy*, vol. 2013 (2013) 827681
- [4] F. Zhang, A. Yamakata, K. Maeda, Y. Moriya, T. Takata, J. Kubota, K. Teshima, S. Oishi, K. Domen, *J. Am. Chem. Soc.*, 134 (2012) 8348
- [5] M. Mori, H. Kagawa, Y. Saito, *Acta Astronautica*, 59 (2006) 132
- [6] T. Suzuki, H. Nasu, M. Hughes, S. Mizuno, K. Hasegawa, H. Ito, Y. Ohishi, *J. Non-Cryst. Solids*, 356 (2010) 2344
- [7] T. Suzuki, H. Kawai, H. Nasu, M. Hughes, Y. Ohishi, S. Mizuno, H. Ito, K. Hasegawa, *Opt. Mater.*, 33 (2011) 1952
- [8] C.G. Young, *Appl. Opt.*, 5 (1966) 993

- [9] M. Weksler, J. Shwartz, *J. Quant. elect.*, 24 (1988) 1222
- [10] H. Arashi, Y. Oka, N. Sasahara, A. Kanai, M. Ishigame, *Jap. J. Appl. Phys.*, 23 (1984) 1051
- [11] T. Yabe, T. Ohkubo, S. Uchida, K. Yoshida, M. Nakatsuka, T. Funatsu, A. Mabuti, A. Oyama, K. Nakagawa, T. Oishi, K. Daito, B. Behgol, Y. Nakayama, M. Yoshida, S. Motokoshi, Y. Sato, C. Baasandash, *Appl. Phys. Lett.*, 90 (2007) 261120, doi: 10.1063/1.2753119
- [12] T. Saiki, M. Nakatsuka, K. Imasaki, *Jap. J. Appl. Phys.*, 49 (2010) 082702
- [13] S.Q. Li, S.H. Zhou, P. Wang, Y.C. Chen, K.K. Lee, *Opt. Lett.*, Vol. 18, No. 3 (1993) 203
- [14] J.P. Oudalov, A. Daoudi, J.C. Joubert, G.L. Flem, P. Hagenmuller, *Bull. Soc. Chim. Fr.*, 10 (1970) 3408
- [15] H.R. Verdun, L.M. Thomas, *Appl. Phys. Lett.*, 56 (1990) 608
- [16] D.H. Cong, D.Y. Tang, W.D. Tan, J. Zhang, D.W. Luo, C.W. Xu, X.D. Xu, D.Z. Li, J. Xu, X.Y. Zhang, Q.P. Wang, *Opt. Comm.*, 286 (2011) 1967
- [17] D.Z. Li, X.D. Xu, J. Meng, D.H. Zhou, C. Xia, F. Wu, J. Xu, *Optics Express*, 18 (2010) 18649
- [18] W.Y. Wang, X.L. Yan, X. Wu, Z.G. Zhang, B.Q. Hu, J.F. Zhou, *J. Cryst. Growth*,

219 (2000) 56

[19] J.Q. Di, X.D. Xu, C.T. Xia, D.Z. Li, D.H. Zhou, Q.L. Sai, L. Wang, J. Xu, *Physica*

B: Condens. Matter, 408 (2013) 1

[20] S.Z. Lv, Z.J. Zhu, Y. Wang, Z.Y. You, J.F. Li, C.Y. Tu, *J. Lumin.*, 144 (2013) 117

[21] J.A. Hutchnson, H.R. Verdun, B.H.T. Chai, B. Zandi, L.D. Merkle, *Opt. Mater.*, 3

(1994) 287

[22] M. Yamaga, P.I. Macfarlane, K. Holliday, B. Henderson, N. Kodama, Y. Inoue, *J.*

Phys.: Condens. Matter, 8 (1996) 3487

[23] T. Stoyanova Lyubenova, J.B. Carda, M. Ocana, *J. Eur. Ceram. Soc.*, 29 (2009)

2193

[24] Yu.P. Udalov, Z. S. Appen, V.V. Parshina, *Zh. Neorg. Khim.*, 24 (1979) 2786;

Russ. J. Inorg. Chem. (Engl. Transl.), 24 (1979) 1549.

Table 1

Compositions of feed rods used for growth experiments.

Sample	Composition
Stoichiometry	$\text{Ca}(\text{Y}_{0.99}\text{Nd}_{0.01})(\text{Al}_{0.999}\text{Cr}_{0.001})\text{O}_4$
Y-rich 0.5 mol% vs. Ca	$\text{Ca}_{0.9925}(\text{Y}_{0.99}\text{Nd}_{0.01})_{1.005}(\text{Al}_{0.999}\text{Cr}_{0.001})\text{O}_4$
Al-rich 0.5 mol% vs. Y	$\text{Ca}(\text{Y}_{0.99}\text{Nd}_{0.01})_{0.995}(\text{Al}_{0.999}\text{Cr}_{0.001})_{1.005}\text{O}_4$

Table 2

Lattice parameters of the initial and end portions of the grown crystal.

Lattice parameter		
	a-axis [\AA]	c-axis [\AA]
Initial portion	3.6455(2)	11.8750(6)
End portion	3.6471(2)	11.8813(6)

Figure captions

Fig. 1 Crystal structure of CaYAlO_4 .

Fig. 2 Cr,Nd:CaYAlO_4 crystals grown under different atmospheres; a: O_2 ; b: air; c: mixed gas ($\text{N}_2/\text{air} = 9/1$); d: N_2 . All crystals were grown at 2.5 mm/h and 30 rpm.

Fig. 3 Polarizing microphotographs of the of the initial portions of the Cr,Nd:CaYAlO_4 crystals grown under different atmospheres. a: O_2 ; b: air; c: mixed gas ($\text{N}_2/\text{air} = 9/1$); d: N_2 . All crystals were grown at 2.5 mm/h and 30 rpm.

Fig. 4 Polarizing microphotographs of the end portions of the Cr,Nd:CaYAlO_4 crystals grown at different growth rates and rotation rates. a: 5 mm/h, 30 rpm; b: 2.5 mm/h, 30 rpm; c: 2.5 mm/h, 60 rpm. All crystals were grown in air.

Fig. 5 Schematic phase diagram in which the stoichiometric composition and the congruent one are different. If the congruent composition is shifted from the stoichiometric one towards an end member, the ionic radius of which is smaller than that of the counter ion, the lattice parameter will increase.

Fig. 6 Polarizing microphotographs of the end portions of the Cr,Nd:CaYAlO_4 crystals grown from feed rods with different compositions. a: Al-rich

composition (Y/Al = 0.995/1.005); b: Y-rich composition (Ca/Y = 0.9925/1.005). Compare the qualities with that of the stoichiometric one shown in Fig. 4b. Every crystal was grown at 2.5 mm/h and 30 rpm in air.

Fig. 7 Polarized absorption spectra of the Cr,Nd:CaYAlO₄ single crystal.

Fig. 8 Emission spectrum of the Cr,Nd:CaYAlO₄ single crystal with the excitation at 400 nm.

Fig. 9 Fluorescence decay curve of 1078 nm emission of Cr,Nd:CaYAlO₄ at room temperature. Excited wavelength was 370 nm, where only absorption fo Cr³⁺ is present.